Joint Beamforming and Mode Selection Design for Hybrid RIS Assisted Integrated Sensing and Communications

Rui Zhao*, Xiaoyan Hu†, Chaowen Liu*, Han Xiao†, Tong-Xing Zheng†, Kai-Kit Wong‡, Guangyue Lu*
*Xi'an University of Posts and Telecommunications, Xi'an, 710121, China
†Xi'an Jiaotong University, Xi'an 710049, China
‡University College London, London WC1E7JE, UK
Email: zhaorui@stu.xupt.edu.cn, xiaoyanhu@xjtu.edu.cn, liucw@xupt.edu.cn, hanxiaonuli@stu.xjtu.edu.cn, zhengtx@mail.xjtu.edu.cn, kai-kit.wong@ucl.ac.uk, tonylugy@163.com

***Abstract*—In this paper, we investigate a hybrid reconfigurable intelligent surface (RIS) enabled integrated sensing and communication (ISAC) system, in which a hybrid RIS is employed to assist a base station (BS) to sense a specified target, while interacting with multiple communication users (CUs) simultaneously. In particular, a hybrid RIS is introduced such that each of its surface module is able to switch between active and passive modes, reducing the system's power consumption. Subsequently, an optimization problem is formulated with the aim of maximizing the radar output signal-to-noise ratio while satisfying communication requirement for each CU, transmit power constraint for BS and the active RIS elements, by jointly optimizing radar recieve filter, BS's transmit beamforming matrix, RIS reflection coefficients, and the selection matrix that determines the working modes for each unite of the hybrid RIS. Since this design problem is not convex, we propose an alternating optimization based method to solve this problem. Eventually, upon the simulation analysis, we demonstrate that the performance achievable by the proposed scheme is significantly better than the counterparts assisted solely by the active or passive RIS.**

***Index Terms*—Hybrid reconfigurable intelligent surface, integrated sensing and communication, joint beamforming and mode selection, block coordinate descent.**

I. Introduction

As a prominent technology in next-generation wireless networks, integrated sensing and communication (ISAC) integrates the traditionally separated functionalities of sensing and communication into one system. Unlike the traditional method of allocating spectrum resources, ISAC enables the transmission beams to possess both communication and radar perception functionality. This integration goes beyond mere spectrum sharing, thereby facilitating seamless collaboration and synergy between the two systems. In recent years, ISAC has garnered significant research interest due to its high efficiency at a low cost [1]- [2].

Reconfigurable intelligent surface (RIS) can serve as a promising technology to expand the propagation range of signals by independently adjusting it to establish reliable non-line-of-sight (NLoS) connections between transmitters and receivers [3]- [4]. By leveraging RIS technology, the ISAC system can effectively surmount obstacles and improve connectivity in challenging NLoS scenarios, thereby enhancing the overall communication performance of the system [5]- [6].

By incorporating active elements into the conventional RIS [7], active RIS is empowered with signal amplification, and is hence capable of combating multiplicative fading, making it especially useful in rapidly changing communication environments [8]. Owing to this, attentions have been put on integrating active RIS with ISAC system. However, due to the additional power consumption required by active RIS, in some cases, passive RIS actually has better performance in some cases [9]- [10]. Existing research encompasses RIS that combine both active and passive elements to support performance-enhanced system designs within the framework of ISAC [11].

By contrast, in this work, we propose to investigate a mode-selective hybrid RIS, with each of its elements being able to switch between active and passive mode, while consider the overall ISAC performance enhanced design. Specifically, in our work, a multi-antenna base station (BS) leverages the assistance of a mode-adaptive hybrid RIS to enhance both communication with multiple single antenna communication users (CUs) and detection of individual sensing target. Our objective is to maximize radar detection performance while satisfying each CU signal-to-interference-and-noise ratio (SINR) constraint, the constraints of BS transmission and hybrid RIS power, and modulus constraints of RIS. We propose to jointly design the transmit beamforming, the radar receive filter, the hybrid RIS reflection coefficients, and the selection matrix of the hybrid RIS determining whether each element works in active or passive mode. The optimization problem established based on the above considerations is a non-convex problem. Afterwards, efficient algorithms based on semi-definite relaxation (SDR), Dinkelbach's transform, majorization-minimization (MM) method and block coordinate descent (BCD) methods [12] are developed to alterna-

This work is partially supported by the Key Research and Development Projects of Shaanxi Province under Grants 2023-YBGY-272 and 2023-YBGY-040, the National Natural Science Foundation of China under Grants 62201449 and 61901366, the Qin Chuang Yuan High-Level Innovation and Entrepreneurship Talent Program under Grant QCYRCXM-2022-231, and the "Si Yuan Scholar" Foundation.

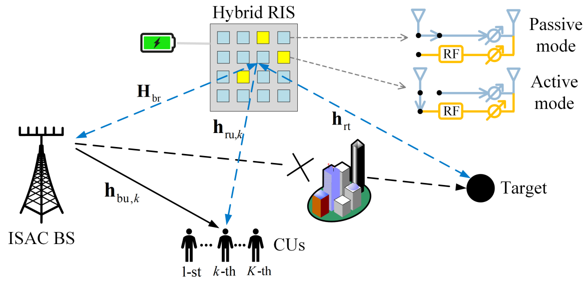

Fig. 1: An illustration of system model.

tively solve them. Simulation studies demonstrate that the deployment of mode-selective hybrid RIS can offer significant sensing performance improvement compared with passive or active RIS-assisted ISAC system.

II. System Model and Problem Formulation

We consider a hybrid RIS-assisted ISAC system serving K single-antenna CUs and one sensing target. The ISAC BS is equipped with M antennas, and the hybrid RIS has N elements. We assume that the detection echo from the target does not interfere with the CUs. The system is illustrated in Fig.1. We use $\mathbf{C}$ and $\mathbf{S}$ to denote beamforming matrices for communication and sensing, respectively, which is $\mathbf{C} = [\mathbf{c}_1, \mathbf{c}_2, \dots, \mathbf{c}_K] \in \mathbb{C}^{M\times K}$, $\mathbf{S} = [\mathbf{s}_1, \mathbf{s}_2, \dots, \mathbf{s}_M] \in \mathbb{C}^{M\times M}$. $\mathbf{d} = [d_1, d_2, \dots, d_K]^T \in \mathbb{C}^{K\times 1}$, $\mathbf{t} = [t_1, t_2, \dots, t_M]^T \in \mathbb{C}^{M\times 1}$ represent signals of communication and sensing respectively. Therefore, the transmitted signal of the BS $\mathbf{x} \in \mathbb{C}^{M\times 1}$ can be given by

$$\mathbf{x} = \mathbf{Cd} + \mathbf{St} = \mathbf{Ws}^{+}, \tag{1}$$

where $\mathbf{W} = [\mathbf{C}\ \mathbf{S}] \in \mathbb{C}^{M\times(K+M)}$ denotes the aggregated beamforming matrix, $\mathbf{s}^{+} = [\mathbf{d}^T\ \mathbf{t}^T]^T \in \mathbb{C}^{(K+M)\times 1}$ denotes the conjuncted sensing and communication signals. Without loss of generality, we assume that the signals are uncorrelated with each other and have unit average power, i.e., $\mathbb{E}[\mathbf{dd}^H] = \mathbf{I}_K$, $\mathbb{E}[\mathbf{tt}^H] = \mathbf{I}_M$ and $\mathbb{E}[\mathbf{dt}^H] = \mathbf{0}$. As a result, the corresponding transmit covariance matrix is given by $\mathbf{R} = \mathbb{E}[\mathbf{xx}^H]$. Let us denote the RIS reflection coefficients by a diagonal matrix $\boldsymbol{\Phi} = \mathrm{diag}(\boldsymbol{\phi})$, where $\boldsymbol{\phi} = [\phi_1, \phi_2, \dots, \phi_N]^T \in \mathbb{C}^{N\times 1}$ is the RIS reflection coefficients vector. The mode selection matrix is denoted by a diagonal matrix $\mathbf{Q}_{\mathrm{a}} = \mathrm{diag}(\mathbf{q})$, [1] where $\mathbf{q}$ is the mode selection vector with its elements $q_n \in [0, 1], n \in \{1, 2, \dots, N\}$. Given $q_n = 0$, the associated RIS element operates passively, i.e., $|\phi_n| = 1$, while $q_n = 1$, the RIS element operates actively, i.e., $|\phi_n| \le \beta_{\max}$. Let $\mathbf{H}_{\mathrm{br}} \in \mathbb{C}^{N\times M}$, $\mathbf{h}_{\mathrm{ru},k} \in \mathbb{C}^{N}$, $\mathbf{h}_{\mathrm{bu},k} \in \mathbb{C}^{M}$, $\mathbf{h}_{\mathrm{rt}} \in \mathbb{C}^{N}$ denote the channels of BS-to-hybrid RIS link, the hybrid RIS-to-k-th CU link, BS-to-k-th CU link and the BS-to-target link respectively. The received signal of k-th CU is modeled as

$$y_k = \mathbf{h}_k^H \mathbf{x} + \mathbf{h}_{\mathrm{ru},k}^H \boldsymbol{\Phi} \mathbf{Q}_{\mathrm{a}} \mathbf{n}_{\mathrm{ris}} + n_k, \tag{2}$$

where $(\mathbf{h}_k = \mathbf{h}_{\mathrm{bu},k} + \mathbf{h}_{\mathrm{ru},k} \boldsymbol{\Phi} \mathbf{H}_{\mathrm{br}}) \in \mathbb{C}^{M\times 1}$ denotes the aggregated channel vector from the BS to k-th CU, $\mathbf{n}_{\mathrm{ris}} \sim \mathcal{CN}(\mathbf{0}, \sigma_{\mathrm{ris}}^2 \mathbf{I})$ is the RIS noise vector incurred by the active RIS, $n_k \sim \mathcal{CN}(0, \sigma_k^2)$ denotes the additive white gaussian noise (AWGN) at k-th CU receiver. The SINR of k-th CU is

$$\gamma_k = \frac{|\mathbf{h}_k^H \mathbf{c}_k|^2}{\sum_{j=1, j\ne k}^{K} |\mathbf{h}_k^H \mathbf{c}_j|^2 + \sum_{m=1}^{M} |\mathbf{h}_k^H \mathbf{s}_m|^2 + z_k(\boldsymbol{\Phi}) + \sigma_k^2}, \tag{3}$$

where, $z_k(\boldsymbol{\Phi}) = \|\mathbf{h}_{\mathrm{ru},k} \boldsymbol{\Phi} \mathbf{Q}_{\mathrm{a}}\|^2 \sigma_{\mathrm{ris}}^2$.

The signals transmitted through BS-to-RIS link and BS-to-RIS-to-target-to-RIS link can be respectively represented as

$$\mathbf{y}_1^{\mathrm{r}} = \boldsymbol{\Phi} \mathbf{H}_{\mathrm{br}} \mathbf{x} + \boldsymbol{\Phi} \mathbf{Q}_{\mathrm{a}} \mathbf{n}_{\mathrm{ris}}, \tag{4a}$$

$$\begin{aligned} \mathbf{y}_2^{\mathrm{r}} = &\alpha \boldsymbol{\Phi}^H \mathbf{h}_{\mathrm{rt}} \mathbf{h}_{\mathrm{rt}}^H \boldsymbol{\Phi} \mathbf{H}_{\mathrm{br}} \mathbf{x} + \alpha \mathbf{Q}_{\mathrm{a}}^H \boldsymbol{\Phi}^H \mathbf{h}_{\mathrm{rt}} \mathbf{h}_{\mathrm{rt}}^H \boldsymbol{\Phi} \mathbf{Q}_{\mathrm{a}} \mathbf{n}_{\mathrm{ris}} \\ &+ \mathbf{Q}_{\mathrm{a}}^H \boldsymbol{\Phi}^H \mathbf{n}_{\mathrm{ris}}, \end{aligned} \tag{4b}$$

where α is the complex-valued amplitude of the radar cross-section (RCS), $\mathbb{E}[|\alpha|^2] = \varsigma^2$. Additionally, as a result of incorporating active components, the hybrid RIS exhibits power consumption. We define $\mathbf{y}_1^{\mathrm{r}*}$ and $\mathbf{y}_2^{\mathrm{r}*}$ as the results of multiplying $\boldsymbol{\Phi}$ and $\mathbf{Q}_{\mathrm{a}}$ with the first element of $\mathbf{y}_1^{\mathrm{r}}$ and $\mathbf{y}_2^{\mathrm{r}}$, respectively, while leaving the remaining elements unchanged. The signal power output from the active RIS elements when detecting the target can be denoted as

$$P^{\mathrm{ris}} = \mathbb{E}\left[\|\mathbf{y}_1^{\mathrm{r}*}\|_2^2 + \|\mathbf{y}_2^{\mathrm{r}*}\|_2^2\right]. \tag{5}$$

By substituting $\mathbf{y}_1^{\mathrm{r}*}$ and $\mathbf{y}_2^{\mathrm{r}*}$ into (5), we have

$$\begin{aligned} P^{\mathrm{ris}} = &\|\boldsymbol{\Phi} \mathbf{Q}_{\mathrm{a}} \mathbf{H}_{\mathrm{br}} \mathbf{W}\|_F^2 + 2\sigma_{\mathrm{ris}}^2 \|\boldsymbol{\Phi} \mathbf{Q}_a\|^2 \\ &+ \underbrace{\|\varsigma^2 \mathbf{Q}_{\mathrm{a}}^H \boldsymbol{\Phi}^H \mathbf{h}_{\mathrm{rt}} \mathbf{h}_{\mathrm{rt}}^H \boldsymbol{\Phi} \mathbf{Q}_{\mathrm{a}} \mathbf{H}_{\mathrm{br}} \mathbf{W}\|_F^2}_{C_1} \\ &+ \underbrace{\|\varsigma^2 \sigma_{\mathrm{ris}}^2 \mathbf{Q}_{\mathrm{a}}^H \boldsymbol{\Phi}^H \mathbf{h}_{\mathrm{rt}} \mathbf{h}_{\mathrm{rt}}^H \boldsymbol{\Phi} \mathbf{Q}_{\mathrm{a}}\|_F^2}_{C_2}. \end{aligned} \tag{6}$$

Consequently, the received echo of radar is expressed as

$$\begin{aligned} \mathbf{y}_{\mathrm{r}} &= \mathbf{H}_{\mathrm{br}}^H (\mathbf{y}_1^{\mathrm{r}} + \mathbf{y}_2^{\mathrm{r}}) + \mathbf{n}_{\mathrm{r}} \\ &= \alpha \mathbf{H}_{\mathrm{br}}^H (\boldsymbol{\Phi}^H \mathbf{h}_{\mathrm{rt}} \mathbf{h}_{\mathrm{rt}}^H \boldsymbol{\Phi} \mathbf{H}_{\mathrm{br}} \mathbf{x} + \mathbf{Q}_{\mathrm{a}}^H \boldsymbol{\Phi}^H \mathbf{h}_{\mathrm{rt}} \mathbf{h}_{\mathrm{rt}}^H \\ &\quad \boldsymbol{\Phi} \mathbf{Q}_{\mathrm{a}}^H \mathbf{n}_{\mathrm{ris}}) + \mathbf{H}_{\mathrm{br}}^H (\boldsymbol{\Phi} \mathbf{Q}_{\mathrm{a}} \mathbf{n}_{\mathrm{ris}} + \mathbf{Q}_{\mathrm{a}}^H \boldsymbol{\Phi}^H \mathbf{n}_{\mathrm{ris}}) + \mathbf{n}_{\mathrm{r}}, \end{aligned} \tag{7}$$

where $\mathbf{n}_{\mathrm{r}} \sim \mathcal{CN}(\mathbf{0}_M, \sigma_{\mathrm{r}}^2 \mathbf{I}_M)$ is AWGN. After postprocessing the received signal $\mathbf{y}_{\mathrm{r}}$ with a receive filter $\mathbf{u} \in \mathbb{C}^M$, the radar output signal at the BS is written as

$$\mathbf{u}^H \mathbf{y}_{\mathrm{r}} = \mathbf{u}^H (\alpha \mathbf{H}_{\mathrm{t}} \mathbf{x} + \mathbf{H}_{\mathrm{t},0} \mathbf{n}_{\mathrm{ris}} + \mathbf{u}^H \mathbf{H}_{\mathrm{t},1} \mathbf{n}_{\mathrm{ris}} + \mathbf{n}_{\mathrm{r}}), \tag{8}$$

where $\mathbf{H}_{\mathrm{t}} \triangleq \mathbf{H}_{\mathrm{br}}^H \boldsymbol{\Phi} \mathbf{h}_{\mathrm{rt}} \mathbf{h}_{\mathrm{rt}}^H \boldsymbol{\Phi}^H \mathbf{H}_{\mathrm{br}}$, $\mathbf{H}_{\mathrm{t},0} \triangleq \mathbf{H}_{\mathrm{br}}^H \boldsymbol{\Phi} \mathbf{Q}_{\mathrm{a}} \mathbf{h}_{\mathrm{rt}} \mathbf{h}_{\mathrm{rt}}^H \mathbf{Q}_{\mathrm{a}}^H \boldsymbol{\Phi}^H$, $\mathbf{H}_{\mathrm{t},1} \triangleq \mathbf{H}_{\mathrm{br}}^H (\boldsymbol{\Phi} \mathbf{Q}_{\mathrm{a}} + \mathbf{Q}_{\mathrm{a}}^H \boldsymbol{\Phi}^H)$. Then, the radar output signal-to-noise ratio (SNR) is obtained as

$$\gamma_{\mathrm{r}} = \frac{\varsigma^2 \mathbf{u}^H \mathbf{H}_{\mathrm{t}} \mathbf{W} \mathbf{W}^H \mathbf{H}_{\mathrm{t}}^H \mathbf{u}}{\mathbf{u}^H (\varsigma^2 \sigma_{\mathrm{ris}}^2 \mathbf{H}_{\mathrm{t},0} \mathbf{H}_{\mathrm{t},0}^H + \sigma_{\mathrm{ris}}^2 \mathbf{H}_{\mathrm{t},1} \mathbf{H}_{\mathrm{t},1}^H + \sigma_{\mathrm{r}}^2 \mathbf{I}_N) \mathbf{u}}. \tag{9}$$

In this paper, we aim to jointly design radar receive filter $\mathbf{u}$, the transmit beamforming $\mathbf{W}$, the hybrid RIS reflection coefficient $\boldsymbol{\phi}$, and the selection matrix $\mathbf{Q}_{\mathrm{a}}$ to maximize the radar SNR, while satisfying the CUs' quality of service (QoS) requirements γ_k, the power budgets $P_{\max}^{\mathrm{BS}}$ at the BS and the hybrid RIS budgets $P_{\max}^{\mathrm{ris}}$. Therefore, the optimization problem is originally formulated as

$$\mathbf{P0} \quad \max_{\mathbf{u}, \mathbf{R}, \mathbf{C}_1, \dots, \mathbf{C}_K, \boldsymbol{\Phi}, \mathbf{q}} \quad \gamma_{\mathrm{r}} \tag{10a}$$

$$\text{s.t.} \quad \mathbf{R} = \mathbf{CC}^H + \mathbf{SS}^H, \mathbf{R} \succeq 0, \mathrm{Tr}(\mathbf{R}) \le P_{\max}^{\mathrm{BS}}, \tag{10b}$$

$$\mathbf{C}_k \succeq 0, \mathrm{rank}(\mathbf{C}_k) = 1, \tag{10c}$$

$$\gamma_k \ge \Gamma_k, \forall k \in \{1, \dots, K\}, \tag{10d}$$

$$P^{\mathrm{ris}} \le P_{\max}^{\mathrm{ris}}, \tag{10e}$$

$$|\phi_n| = 1, q_n = 0, \tag{10f}$$

$$|\phi_n| \le \beta_{\max}, q_n = 1, \tag{10g}$$

[1]The functionality of $\mathbf{Q}_{\mathrm{a}}$ is to multiply with the reflection coefficient matrix, select the elements in the active state, and calculate additional power consumption or noise they introduce.

where (10b) is the the constraint of the total transmitted power of BS. (10d) represents the SINR constraint of the k-th CU. (10e) signifies the power budget constraint of the hybrid RIS. (10f) and (10g) represent two situations with regard to $q_n = 1$ and $q_n = 0$ respectively.

III. Proposed Solution For Hybrid-RIS Assisted ISAC Design

In this section, we establish the overall solution framework upon employing the BCD method, which divides the problem into three sub-problems of optimizing variables $\{\mathbf{u}\}$, $\{\mathbf{R}, \mathbf{C}_k\}$, $\{\mathbf{\Phi}, \mathbf{q}\}$. The first sub-problem is solved using the Rayleigh quotient method, which yields a closed-form solution. The second sub-problem is addressed by applying the SDR approach. Finally, the third sub-problem is tackled utilizing the Dinkelbach's transform and MM methods.

A. Design of Radar Receive Filter $\mathbf{u}$ *With Given* $\{\mathbf{C}_k\}_{k=1}^K$, $\mathbf{R}$, $\mathbf{\Phi}$ *And* $\mathbf{q}$

Given transmission beamforming $\mathbf{W}$ of BS and hybrid RIS reflection coefficients ϕ, as well as the selection matrix $\mathbf{Q}_\mathrm{a}$. To enhance the conciseness of the expression, we define

$$\mathbf{A} = \varsigma^2 \mathbf{H}_\mathrm{t} \mathbf{W}\mathbf{W}^H \mathbf{H}_\mathrm{t}^H, \tag{11a}$$

$$\mathbf{B} = \varsigma^2 \sigma_\mathrm{ris}^2 \mathbf{H}_{\mathrm{t},0} \mathbf{H}_{\mathrm{t},0}^H + \sigma_\mathrm{ris}^2 \mathbf{H}_{\mathrm{t},1} \mathbf{H}_{\mathrm{t},1}^H + \sigma_\mathrm{r}^2 \mathbf{I}_N. \tag{11b}$$

Accordingly, The optimization problem of solving for the radar receiver filter $\mathbf{u}$ can be represented as

$$\mathbf{P1} \quad \max_{\mathbf{u}} \quad \frac{\varsigma^2 \mathbf{u}^H \mathbf{A}\mathbf{u}}{\mathbf{u}^H \mathbf{B}\mathbf{u}}. \tag{12}$$

It is worth to note that problem **P1** can be identified as a typical generalized Rayleigh quotient, and its optimal solution is the eigenvector associated with the largest eigenvalue of the matrix obtained by $\mathbf{B}^{-1}\mathbf{A}$. This result is well-known in the theory of generalized eigenvalue problems.

B. Design of BS's Transmit Beamforming $\{\mathbf{C}_k\}_{k=1}^K$, $\mathbf{R}$ *With Given* $\mathbf{u}$, $\mathbf{\Phi}$ *And* $\mathbf{q}$

To solve the initial subproblem, we first reformulate redefine the communication and sensing beamforming at BS upon introducing a rank-1 matrix. The rank-1 matrix $\mathbf{C}_k$ is obtained by processing each column $\{\mathbf{c}_1, \ldots, \mathbf{c}_K\}$ of $\mathbf{C}$, and can be expressed as $\mathbf{C}_k = \mathbf{c}_k \mathbf{c}_k^H \in \mathbb{C}^{M \times M}, \forall k \in \{1, \ldots, K\}$. The covariance representation of sensing beamforming can be given as $\mathbf{R}_0 = \mathbf{S}\mathbf{S}^H$, also we have $\mathbf{C}\mathbf{C}^H = \sum_{k=1}^K \mathbf{C}_k$. Thus, $\mathbf{R} = \mathbf{R}_0 + \mathbf{C}\mathbf{C}^H = \mathbf{R}_0 + \sum_{k=1}^K \mathbf{C}_k$. (10d) can be converted to $(1+\Gamma^{-1})\mathbf{h}_k^H \mathbf{C}_k \mathbf{h}_k \geq \mathbf{h}_k^H \mathbf{R}\mathbf{h}_k + z_k(\mathbf{\Phi}) + \sigma_k^2, k \in \{1, \ldots, K\}$. (10e) exhibit convex forms with respect to $\mathbf{R}$ or $\mathbf{C}$. Therefore, these two constraints can be directly included as constraints in the convex optimization solver tool. In this circumstance, the joint optimization of ($\{\mathbf{C}_k\}_{k=1}^K$, $\mathbf{R}$) can be simplified as

$$\mathbf{P2} \quad \max_{\mathbf{R}, \{\mathbf{C_1}, \ldots, \mathbf{C_K}\}} \quad \mathrm{Tr}(\mathbf{R}\mathbf{H}_\mathrm{t}\mathbf{u}\mathbf{u}^H\mathbf{H}_\mathrm{t}^H) \tag{13a}$$

$$\text{s.t.} \quad (1+\Gamma^{-1})\mathbf{h}_k^H \mathbf{C}_k \mathbf{h}_k \geq \mathbf{h}_k^H \mathbf{R}\mathbf{h}_k + z_k(\mathbf{\Phi}) + \sigma_k^2, k \in \{1, \ldots, K\}, \tag{13b}$$

$$\text{(10b), (10e).}$$

By dropping the rank-1 constraint, **P2** is a standard SDR [13] which can be solved using off-the-shelf solvers. To recover rank-1 matrices $\mathbf{C}_k$ from the SDR solution, we adopt the procedure described in [1]. Assuming that $\mathbf{R}^*$ and $\mathbf{C}^*$ are the optimal solutions for **P2**, we can construct a rank-1 beamformer as follows

$$\mathbf{c}_k = \frac{\mathbf{C}^* \mathbf{h}_k}{\sqrt{\mathbf{h}_k^H \mathbf{C}^* \mathbf{h}_k}}, \mathbf{C}_k = \mathbf{c}_k \mathbf{c}_k^H. \tag{14}$$

Since (14) satisfies $\mathbf{h}_k^H \mathbf{C}_k \mathbf{h}_k = \mathbf{h}_k^H \mathbf{C}^* \mathbf{h}_k, \forall k$, we then use the Cholesky decomposition to obtain the sensing beamforming as

$$(\mathbf{R}^* - \sum\nolimits_{k=1}^K \mathbf{C}_k) = \mathbf{R}_0. \tag{15}$$

As the solutions obtained by utilizing (14) and (15) are feasible solutions to **P2**, we can obtained the optimal solutions for the problem before relaxation.

C. Design of RIS's Reflection Coefficient $\mathbf{\Phi}$, *Mode Selection Matrix* $\mathbf{q}$ *With Given* $\mathbf{u}, \{\mathbf{C}_k\}_{k=1}^K$ *and* $\mathbf{R}$

Given the presence of higher-order terms involving $\mathbf{\Phi}$ and $\mathbf{q}$ in (6), (9), it is necessary to establish a preliminary definition $\mathbf{x} \triangleq \mathrm{vec}(\boldsymbol{\phi}^\mathrm{H}\boldsymbol{\phi}) = \boldsymbol{\phi} \otimes \boldsymbol{\phi}$, $\mathbf{x}_\mathrm{a} \triangleq \mathrm{vec}(\boldsymbol{\phi}_\mathrm{a}^\mathrm{H}\boldsymbol{\phi}_\mathrm{a}) = \boldsymbol{\phi}_\mathrm{a} \otimes \boldsymbol{\phi}_\mathrm{a}$, where $\mathrm{diag}(\boldsymbol{\phi}_\mathrm{a}) = \mathbf{\Phi}_\mathrm{a} = \mathbf{\Phi}\mathbf{Q}_\mathrm{a}$. To address the optimization problem involving $\mathbf{\Phi}$ and $\mathbf{q}$, we can initially represent the objective function as a fraction with a numerator in terms of $\boldsymbol{\phi}$ and a denominator in terms of $\boldsymbol{\phi}_\mathrm{a}$. This can be formulated as $\gamma_\mathrm{r} = f(\boldsymbol{\phi})/g(\boldsymbol{\phi})$, where

$$f(\boldsymbol{\phi}) \triangleq \varsigma^2 \mathbf{u}^H \mathbf{H}_\mathrm{t} \mathbf{W}\mathbf{W}^H \mathbf{H}_\mathrm{t}^H \mathbf{u}, \tag{16a}$$

$$g(\boldsymbol{\phi}) \triangleq \mathbf{u}^H (\varsigma^2 \sigma_\mathrm{ris}^2 \mathbf{H}_{\mathrm{t},0} \mathbf{H}_{\mathrm{t},0}^H + \sigma_\mathrm{ris}^2 \mathbf{H}_{\mathrm{t},1} \mathbf{H}_{\mathrm{t},1}^H + \sigma_\mathrm{r}^2 \mathbf{I}_N)\mathbf{u}. \tag{16b}$$

Then, the subproblem of designing $\mathbf{\Phi}, \mathbf{q}$ can be expressed as

$$\mathbf{P3} \quad \max_{\boldsymbol{\phi}, \boldsymbol{q}} \quad f(\boldsymbol{\phi})/g(\boldsymbol{\phi}) \tag{17}$$

$$\text{s.t.} \quad \text{(10d)-(10g).}$$

Initially, we employ Dinkelbach's transform to address the fraction. Following Dinkelbach's transform, we introduce an auxiliary variable ω and express the first term of the fraction as an optimization problem.

$$\begin{aligned} &\max_{\omega} \quad \omega \\ &\text{s.t.} \quad f(\boldsymbol{\phi}) - \omega \cdot g(\boldsymbol{\phi}) \geq 0, \quad \omega \geq 0. \end{aligned} \tag{18}$$

It is evident that the optimal solution to this problem is

$$\omega^* = f(\boldsymbol{\phi})/g(\boldsymbol{\phi}). \tag{19}$$

By employing the transformation $\mathbf{\Phi}\mathbf{h}_\mathrm{rt} = \mathrm{diag}\{\mathbf{h}_\mathrm{rt}\}\boldsymbol{\phi}$, $\mathrm{Tr}(\mathbf{ABCD}) = \mathrm{vec}^H\{\mathbf{D}\}(\mathbf{C}^T \otimes \mathbf{A})\mathrm{vec}\{\mathbf{B}\}$ and defining $\mathbf{J} = \mathbf{H}_\mathrm{br}^H \mathrm{diag}\{\mathbf{h}_\mathrm{rt}\}$, $f(\boldsymbol{\phi})$ can be reexpressed as

$$\begin{aligned} f(\boldsymbol{\phi}) =& \varsigma^2 \mathbf{u}^H \mathbf{J}\boldsymbol{\phi}^H \boldsymbol{\phi} \mathbf{J}^H \mathbf{W}\mathbf{W}^H \mathbf{J}\boldsymbol{\phi}^H \boldsymbol{\phi} \mathbf{J}^H \mathbf{u} \\ =& \varsigma^2 \mathrm{Tr}\{\mathbf{J}^H \mathbf{u}\mathbf{u}^H \mathbf{J}\boldsymbol{\phi}^H \boldsymbol{\phi} \mathbf{J}^H \mathbf{W}\mathbf{W}^H \mathbf{J}\boldsymbol{\phi}^H \boldsymbol{\phi}\} \\ =& \mathbf{x}^H \mathbf{G}\mathbf{x}, \end{aligned} \tag{20}$$

where $\mathbf{G} = \varsigma^2 (\mathbf{J}^H \mathbf{W}\mathbf{W}^H \mathbf{J})^T \otimes (\mathbf{J}^H \mathbf{u}\mathbf{u}^H \mathbf{J})$. Using the similar derivations in (20), we can reformulate $g(\boldsymbol{\phi})$ as

$$g(\boldsymbol{\phi}) = \mathbf{x}_\mathrm{a}^H \mathbf{D}\mathbf{x}_\mathrm{a} + \boldsymbol{\phi}_\mathrm{a}^H \mathbf{E}\boldsymbol{\phi}_\mathrm{a} + \sigma_\mathrm{r}^2 \|\mathbf{u}\|_2^2, \tag{21}$$

where, $\mathbf{D} \triangleq \varsigma^2 \sigma_\mathrm{ris}^2 (\mathrm{diag}\{\mathbf{h}_\mathrm{rt}\}\mathrm{diag}\{\mathbf{h}_\mathrm{rt}^H\}) \otimes (\mathbf{J}^H \mathbf{u}\mathbf{u}^H \mathbf{J})$, $\mathbf{E} \triangleq 4\sigma_\mathrm{ris}^2 \mathrm{diag}\{\mathbf{u}^H \mathbf{H}_\mathrm{br}^H\}\mathrm{diag}\{\mathbf{u}\mathbf{H}_\mathrm{br}\}$. Then, we have the reformulated objective function of $(\omega g(\boldsymbol{\phi}) - f(\boldsymbol{\phi}))$ as

$$\min_{\boldsymbol{\phi}} \quad -\mathbf{x}^H \mathbf{G}\mathbf{x} + \omega \mathbf{x}_\mathrm{a}^H \mathbf{D}\mathbf{x}_\mathrm{a} + \omega \boldsymbol{\phi}_\mathrm{a}^H \mathbf{E}\boldsymbol{\phi}_\mathrm{a} + \omega \sigma_\mathrm{r}^2 \|\mathbf{u}\|_2^2, \tag{22}$$

The quartic term $\mathbf{x}^H \mathbf{G}\mathbf{x}$ presents a significant difficulty to be addressed. To cope with this, we introduce the MM's method and seek a suitable surrogate function to reformulate the problem into an explicit form. By utilizing the second-order Taylor expansion, we can obtain an upper-bound approximation for $\mathbf{x}^H\mathbf{G}\mathbf{x}$ at the point of $\mathbf{x}_s$ as

$$\begin{aligned}\mathbf{x}^H\mathbf{G}\mathbf{x} \leq &\lambda_{\mathrm{g}}\mathbf{x}^H\mathbf{x} + 2\Re\{\mathbf{x}^H\left(\mathbf{G} - \lambda_{\mathrm{g}}\mathbf{I}N^2\right)\mathbf{x}_{\mathrm{s}}\} \\ &+ \mathbf{x}_{\mathrm{s}}^H\left(\lambda_{\mathrm{g}}\mathbf{I}_{N^2} - \mathbf{g}\right)\mathbf{x}_{\mathrm{s}},\end{aligned} \tag{23}$$

where λ_{g} is the maximum eigenvalue of matrix $\mathbf{G}$. Rendering the amplitude constraint $\beta \leq \beta_{\max}$ is considered, it becomes evident that the term $\mathbf{x}^H\mathbf{x}$ can be bounded as follows.

$$\begin{aligned}\mathbf{x}^H\mathbf{x} &= (\boldsymbol{\phi}\otimes\boldsymbol{\phi})^H(\boldsymbol{\phi}\otimes\boldsymbol{\phi}) = (\boldsymbol{\phi}^H\boldsymbol{\phi})\otimes(\boldsymbol{\phi}^H\boldsymbol{\phi}) \\ &\leq (N_{\mathrm{a}}\beta_{\max}^2 + (N - N_{\mathrm{a}}))^2.\end{aligned} \tag{24}$$

where N_{a} represents the number of active RIS elements. Substituting the result in (24) into (23), then the upper-bound of $\mathbf{x}^H\mathbf{G}\mathbf{x}$ can be equivalently transformed as

$$\mathbf{x}^H\mathbf{G}\mathbf{x} \leq \Re\{\mathbf{x}^H\mathbf{g}\} + a_1 = \Re\{\boldsymbol{\phi}^H\tilde{\mathbf{G}}\boldsymbol{\phi}\} + a_1, \tag{25}$$

where $\mathbf{g} \triangleq 2(\mathbf{G} - \lambda_{\mathrm{g}}\mathbf{I}_{N^2})\mathbf{x}_{\mathrm{s}}$ and $a_1 \triangleq \lambda_{\mathrm{g}}(N_{\mathrm{a}}\beta_{\max}^2 + (N - N_{\mathrm{a}}))^2 + \mathbf{x}_{\mathrm{s}}^H(\lambda_{\mathrm{g}}\mathbf{I}_{N^2} - \mathbf{G})\mathbf{x}_{\mathrm{s}}$. $\tilde{\mathbf{G}}$ is the reshaped matrix of vector $\mathbf{g}$. Since $\Re\{\boldsymbol{\phi}^H\tilde{\mathbf{G}}\boldsymbol{\phi}\}$ in (25) is still non-convex with respect to $\boldsymbol{\phi}$, we introduce auxiliary variables $\bar{\boldsymbol{\phi}} \triangleq \left[\Re\{\boldsymbol{\phi}^H\}, \Im\{\boldsymbol{\phi}^H\}\right]^H$, $\bar{\mathbf{G}} \triangleq \begin{bmatrix}\Re\{\tilde{\mathbf{G}}\} & \Im\{\tilde{\mathbf{G}}\} \\ \Im\{\tilde{\mathbf{G}}\} & -\Re\{\tilde{\mathbf{G}}\}\end{bmatrix}$. Afterwards, the second-order Taylor expansion of $\bar{\boldsymbol{\phi}}^H\bar{\mathbf{G}}\bar{\boldsymbol{\phi}}$ can be achieved as

$$\begin{aligned}\bar{\boldsymbol{\phi}}^H\bar{\mathbf{L}}\,\bar{\boldsymbol{\phi}} &\leq \bar{\boldsymbol{\phi}}_{\mathrm{s}}^H\bar{\mathbf{G}}\,\bar{\boldsymbol{\phi}}_{\mathrm{s}} + \left(\bar{\boldsymbol{\phi}}_{\mathrm{s}}^H(\bar{\mathbf{G}} + \bar{\mathbf{G}}^H) + \frac{\lambda_{\tilde{\mathrm{g}}}}{2}(\bar{\boldsymbol{\phi}} - \bar{\boldsymbol{\phi}}_{\mathrm{s}})^H\right)(\bar{\boldsymbol{\phi}} - \bar{\boldsymbol{\phi}}_{\mathrm{s}}) \\ &= \frac{\lambda_{\tilde{\mathrm{g}}}}{2}\boldsymbol{\phi}^H\boldsymbol{\phi} + \Re\{\boldsymbol{\phi}^H\tilde{\mathbf{g}}\} + a_2,\end{aligned} \tag{26}$$

where $\lambda_{\tilde{\mathrm{g}}}$ is the maximum eigenvalue of Hessian matrix $(\bar{\mathbf{G}} + \bar{\mathbf{G}}^H)$, $\tilde{\mathbf{g}} \triangleq \mathbf{U}(\bar{\mathbf{G}} + \bar{\mathbf{G}}^H - \lambda_{\tilde{\mathrm{g}}}\mathbf{I}_{2N})\bar{\boldsymbol{\phi}}_{\mathrm{s}}$, $\mathbf{U} \triangleq [\mathbf{I}_N, j\mathbf{I}_N]$, $a_2 \triangleq -\bar{\boldsymbol{\phi}}_{\mathrm{s}}^H\bar{\mathbf{G}}^H\bar{\boldsymbol{\phi}}_{\mathrm{s}} + \frac{\lambda_{\tilde{\mathrm{g}}}}{2}\bar{\boldsymbol{\phi}}_{\mathrm{s}}^H\bar{\boldsymbol{\phi}}_{\mathrm{s}}$. After summarizing the derivations in (24), (25) and (26), we obtain the convex form of (22).

$$\mathbf{x}^H\mathbf{G}\mathbf{x} \leq \frac{\lambda_{\tilde{\mathrm{g}}}}{2}\boldsymbol{\phi}^H\boldsymbol{\phi} + \Re\{\boldsymbol{\phi}^H\tilde{\mathbf{g}}\} + a_1 + a_2. \tag{27}$$

Hence, the objective function of (22) can be converted into

$$\min_{\boldsymbol{\phi}} \quad \boldsymbol{\phi}_{\mathrm{a}}^H\tilde{\mathbf{E}}\boldsymbol{\phi}_{\mathrm{a}} + \Re\{\boldsymbol{\phi}^H\tilde{\mathbf{d}}\} - \Re\{\boldsymbol{\phi}^H\tilde{\mathbf{g}}\} - \frac{\lambda_{\tilde{\mathrm{g}}}}{2}\boldsymbol{\phi}^H\boldsymbol{\phi}, \tag{28}$$

where $\tilde{\mathbf{E}} \triangleq \omega(\mathbf{E} + \frac{\lambda_{\tilde{\mathrm{d}}}}{2}\mathbf{I}_M)$, the transformation operations of $\tilde{\mathbf{d}}$ and $\lambda_{\tilde{d}}$ from $\mathbf{D}$ are similar to those of $\tilde{\mathbf{g}}$ and $\lambda_{\tilde{g}}$ from $\mathbf{G}$.

We can observe that (10e) is still non-convex due to the non-convexity of $C_1 + C_2$. To facilitate problem solving, we extract the variable $\boldsymbol{\phi}_{\mathrm{a}}$ from P^{ris}, and re-write it as

$$P^{\mathrm{ris}} = \mathbf{x}_{\mathrm{a}}^H\mathbf{F}\mathbf{x}_{\mathrm{a}} + \boldsymbol{\phi}_{\mathrm{a}}^H\mathbf{K}\boldsymbol{\phi}_{\mathrm{a}}, \tag{29}$$

where

$$\begin{aligned}\mathbf{F} &= \varsigma^2(\tilde{\mathbf{Q}}^T\otimes(\mathbf{J}^H\mathbf{R}\mathbf{J}), \\ \mathbf{K} &= \sum\nolimits_{k=1}^{K+M}\mathrm{diag}\{\mathbf{H}_{\mathrm{br}}^*\mathbf{w}_k^*\}\mathrm{diag}\{\mathbf{H}_{\mathrm{br}}\mathbf{w}_k\}.\end{aligned} \tag{30}$$

Specifically,

$$\mathbf{x}_{\mathrm{a}}^H\mathbf{x}_{\mathrm{a}} = (\boldsymbol{\phi}_{\mathrm{a}}^H\boldsymbol{\phi}_{\mathrm{a}})\otimes(\boldsymbol{\phi}_{\mathrm{a}}^H\boldsymbol{\phi}_{\mathrm{a}}) \leq (N_{\mathrm{a}}\beta_{\max})^4, \tag{31}$$

for $\mathbf{x}_a^H\mathbf{F}\mathbf{x}_a$, we utilize the same method to convert,

$$\mathbf{x}_{\mathrm{a}}{}^H\mathbf{F}\mathbf{x}_{\mathrm{a}} \leq \frac{\lambda_{\tilde{\mathrm{f}}}}{2}\boldsymbol{\phi}_{\mathrm{a}}^H\boldsymbol{\phi}_{\mathrm{a}} + \Re\{\boldsymbol{\phi}_{\mathrm{a}}^H\tilde{\mathbf{f}}\} + a_5 + a_6, \tag{32}$$

where $\mathbf{f} \triangleq 2(\mathbf{F} - \lambda_{\mathrm{f}}\mathbf{I}_{N^2})\mathbf{x}_{\mathrm{as}} = \mathrm{vec}\{\tilde{\mathbf{F}}\}$, $\tilde{\mathbf{F}}$ is reshaped by $\mathbf{f}$, and $\bar{\mathbf{F}} \triangleq \begin{bmatrix}\Re\{\tilde{\mathbf{F}}\} & \Im\{\tilde{\mathbf{F}}\} \\ \Im\{\tilde{\mathbf{F}}\} & -\Re\{\tilde{\mathbf{F}}\}\end{bmatrix}$,
$a_5 \triangleq \lambda_{\mathrm{f}}(N_{\mathrm{a}}\beta_{\max})^4 + \mathbf{x}_{\mathrm{as}}^H(\lambda_{\mathrm{f}}\mathbf{I}_{N^2} - \mathbf{F})\mathbf{x}_{\mathrm{as}}$,
$a_6 \triangleq -\bar{\boldsymbol{\phi}}_{\mathrm{as}}^T\bar{\mathbf{F}}^T\bar{\boldsymbol{\phi}}_{\mathrm{as}} + \lambda_{\tilde{\mathrm{f}}}\bar{\boldsymbol{\phi}}_{\mathrm{as}}^T\bar{\boldsymbol{\phi}}_{\mathrm{as}}$,
$\lambda_{\tilde{\mathrm{f}}}$ is the maximum eigenvalue of Hessian matrix $(\bar{\mathbf{F}} + \bar{\mathbf{F}}^T)$, $\lambda_{\mathrm{f}} = \mathrm{Tr}\{\mathbf{F}\}$, $\tilde{\mathbf{f}} \triangleq \mathbf{U}(\bar{\mathbf{F}} + \bar{\mathbf{F}}^T - \lambda_{\mathrm{f}}\mathbf{I}_{2N})\bar{\boldsymbol{\phi}}_{\mathrm{as}}$.

As a result, we can obtain the upper bound of P^{ris} as

$$P_1^{\mathrm{ris}} = \boldsymbol{\phi}_{\mathrm{a}}^H\mathbf{K}\boldsymbol{\phi}_{\mathrm{a}} + \frac{\lambda_{\tilde{\mathrm{f}}}}{2}\boldsymbol{\phi}_{\mathrm{a}}^H\boldsymbol{\phi}_{\mathrm{a}} + \Re\{\boldsymbol{\phi}_{\mathrm{a}}^H\tilde{\mathbf{f}}\} + a_5 + a_6. \tag{33}$$

where $\tilde{\mathbf{K}} \triangleq \mathbf{K} + \frac{\lambda_{\tilde{\mathrm{f}}}}{2}\mathbf{I}_N$. The communication SINR constraint (10d) can be converted into

$$\sqrt{1 + \Gamma_k}\,|\tilde{a}_k(\boldsymbol{\phi})| \geq \sqrt{\Gamma_k}\left\|\tilde{\mathbf{b}}_k(\boldsymbol{\phi})\right\|_2, \forall k, \tag{34}$$

where

$$\tilde{a}_k(\boldsymbol{\phi}) \triangleq \mathbf{h}_{\mathrm{bu},k}^H\mathbf{c}_k + \mathbf{h}_{\mathrm{ru},k}^H\mathrm{diag}(\mathbf{H}_{\mathrm{br}}\mathbf{c}_k)\boldsymbol{\phi}, \tag{35a}$$

$$\tilde{\mathbf{b}}_k(\boldsymbol{\phi}) \triangleq \begin{bmatrix}\mathbf{a}_k + \mathbf{B}_k^H\boldsymbol{\phi} \\ \mathbf{o}_k + \mathbf{P}_k^H\boldsymbol{\phi} \\ \sigma_{\mathrm{ris}}\mathrm{diag}\{\mathbf{h}_{\mathrm{ru},k}\}\boldsymbol{\phi} \\ \sigma_k\end{bmatrix}, \tag{35b}$$

$$\mathbf{a}_k \triangleq \left[\mathbf{h}_{\mathrm{bu},k}^H\mathbf{c}_1 \;\cdots\; \mathbf{h}_{\mathrm{bu},k}^H\mathbf{c}_K\right]^H, \tag{35c}$$

$$\mathbf{B}_k \triangleq \left[\mathrm{diag}\{\mathbf{H}_{\mathrm{br}}\mathbf{c}_1\}\mathbf{h}_{\mathrm{ru},k} \;\cdots\; \mathrm{diag}\{\mathbf{H}_{\mathrm{br}}\mathbf{c}_M\}\mathbf{h}_{\mathrm{ru},k}\right], \tag{35d}$$

$$\mathbf{o}_k \triangleq \left[\mathbf{h}_{\mathrm{bu},k}^H\mathbf{s}_1 \;\cdots\; \mathbf{h}_{\mathrm{bu},k}^H\mathbf{s}_M\right]^H, \tag{35e}$$

$$\mathbf{P}_k \triangleq \left[\mathrm{diag}\{\mathbf{H}_{\mathrm{br}}\mathbf{s}_1\}\mathbf{h}_{\mathrm{ru},k} \;\cdots\; \mathrm{diag}\{\mathbf{H}_{\mathrm{br}}\mathbf{s}_M\}\mathbf{h}_{\mathrm{ru},k}\right]. \tag{35f}$$

Therefore, the optimization for updating $\boldsymbol{\phi}$ is reformulated as

$$\mathbf{P4} \quad \min_{\boldsymbol{\phi},\boldsymbol{\phi}_a} \boldsymbol{\phi}^H\tilde{\mathbf{E}}\boldsymbol{\phi} + \Re\{\boldsymbol{\phi}^H\tilde{\mathbf{l}}\} \tag{36a}$$

$$\text{s.t.} \quad P_1^{\mathrm{ris}} \leq P_{\max}^{\mathrm{ris}}, (34). \tag{36b}$$

The constraint on the variable $\mathbf{q}$ is discrete. Then for simplicity in solving, $\mathbf{q}$ is continuously relaxed to $0 \leq q_n \leq 1, \forall n$. Futher, to facilitate the calculation, we use a fractional expression to represent each element of $\mathbf{q}$, which is shown in (37b), where m_n is 0 or 1, ρ is a constant regulator. The separate cases of $m_n = 0$, $q_n = 0$, while $m_n = 1$, $q_n = 1$, represent passive and active mode of RIS, respectively. The continuous conversions of (10f) and (10g) can be obtained as

$$0 \leq |\phi_n|\,(1 - q_n) \leq 1, 0 \leq |\phi_n|\,q_n \leq \beta_{\max}, \tag{37a}$$

$$q_n = \frac{m_n}{1 + \rho(1 - m_n)}, m_n \in [0, 1], \forall n \in \{1, \ldots, N\}. \tag{37b}$$

Notice that, constraint (37b) is an equality constraint which is not easily handled by optimization solvers. We transform it slightly while multiply it with a penalty factor η, and then added the penalty term to the objective function. Consequently, the optimization for updating $\mathbf{q}$ can be reformulated as

$$\mathbf{P5} \quad \min_{\mathbf{q}} \boldsymbol{\phi}^H\tilde{\mathbf{E}}\boldsymbol{\phi} + \Re\{\boldsymbol{\phi}^H\tilde{\mathbf{l}}\} + \eta\sum_{n=1}^{N}((\rho + 1) - \rho m_n)q_n - m_n \tag{38a}$$

$$\text{s.t.} \quad P_1^{\mathrm{ris}} \leq P_{\max}^{\mathrm{ris}}, (34), (37a). \tag{38b}$$

P4 and **P5** is a convex problem, and thus convex optimization tools can be used to obtain the solution, and an alternating iterative approach is employed within this sub-problem by optimizing one variable while holding another variable constant.

IV. Simulation Results

In this section, we provide simulation results to demonstrate the advancement of the proposed hybrid RIS-assisted ISAC scheme and the effectiveness of the developed joint design algorithm. We set the number of BS antenna to $M = 4$, the number of CUs to $K = 2$, and the noise powers as $\sigma_k^2 = -70$dBm, $\sigma_{\mathrm{ris}}^2 = -63$dBm, $\forall k$, and the RCS as $\varsigma^2 = 1$. We assume that the ISAC BS is equipped with uniform linear arrays (ULAs). We utilize a typical distance dependent path-loss model: $PL(d) = C_0(d_0/d)^\iota$, the distances for the BS-RIS, RIS-CUs and BS-CUs links are set as 10m,

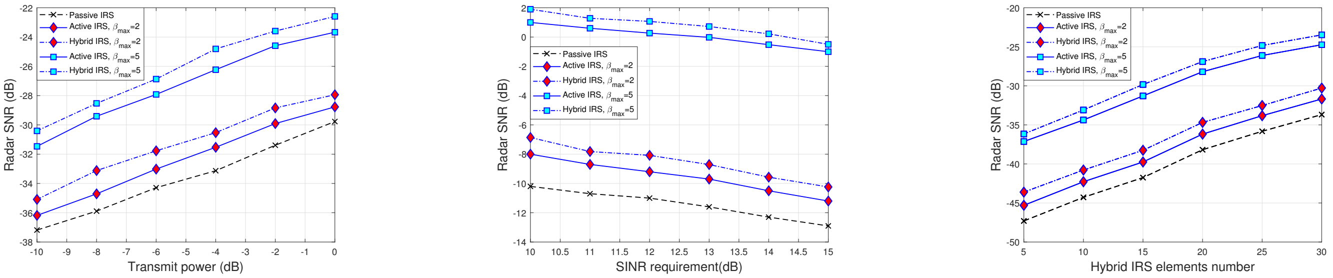

(a) (b) (c)

Fig. 2: (a) Radar SNR versus $P_{\max}^{\rm BS}$: $P_{\max}^{\rm ris} = -3$dB$, N = 6, \Gamma = 10$dB. (b) Radar SNR versus Γ: $P_{\max}^{\rm BS} = 0$dB$, P_{\max}^{\rm ris} = -2dB, N = 6, \Gamma = 10$dB. (c) Radar SNR versus N: $P_{\max}^{\rm BS} = 0$dB$, P_{\max}^{\rm ris} = -3dB, \Gamma = 10$dB.

20m, and 30m, with path-loss exponents of 2.7, 2.8, and 3.0, respectively. The reflected signals from the target to the CUs are disregarded due to severe channel fading. In addition, the channels of the BS-CUs and RIS-CUs links follow the Rayleigh fading model, while the others are LoS.

The radar SNR versus the transmit power budget is first presented in Fig. 2 (a). In order to verify the effectiveness of the proposed hybrid RIS-assisted ISAC scheme, we include the passive RIS-assisted ISAC scheme and the pure active RIS-assisted scheme, with upper limits of the amplification coefficients set at 2 and 5, respectively, for comparison. The transmit power for the passive RIS case is set as $P_{\rm BS}^{\max}+P_{\rm ris}^{\max}$. The amplification factor of the active RIS is positively correlated with the SNR of the radar system. This implies that an increase in the amplification factor leads to a corresponding enhancement in the SNR. The proposed approach is observed to achieve a remarkable improvement in performance compared to the other scheme.

Fig. 2 (b) depicts the radar SNR versus SINR threshold. Improved communication performance with users can lead to a reduction in detection performance, revealing the trade-off between radar and communication performance. The hybrid RIS-assisted scheme proposed in this work demonstrates an approximate 1 dB improvement in performance compared to the performance of the RIS-assisted ISAC scheme.

The radar SNR versus the number of reflection elements N is illustrated in Fig. 2 (c), in accordance with our expectations, the radar SNR increases with the growth in the number of reflecting elements since it provides more DoFs to manipulate wireless environment. In the $\beta_{\max} = 2$ scheme, the hybrid approach achieves an average performance improvement of 1.2 dB compared to the active approach. In the $\beta_{\max} = 5$ scheme, the hybrid approach achieves an average performance improvement of 1.1 dB compared to the active approach in terms of performance.

V. Conclusions

In this paper, we investigated joint beamforming and mode selection design for the hybrid RIS assisted ISAC system. The SNR of the radar echo signal was maximized under each CU SINR constraint, the transmit power constraint, the hybrid RIS power constraint, and the unit modulus restriction on the reflecting coefficients. An efficient algorithm based on BCD methods was developed to convert the resulting non-convex problem into several tractable sub-problems and then iteratively solve them. The simulation results demonstrated the benefits of integrating mode-selective hybrid RIS into ISAC systems, while validated the efficacy of our proposed method.

References

[1] X. Liu, T. Huang, N. Shlezinger *et.al.*, "Joint transmit beamforming for multiuser MIMO communications and MIMO radar," *IEEE Trans. Signal Process*, vol. 68, pp. 3929–3944, 2020.

[2] F. Liu, C. Masouros, and A. P. Petropulu, "Joint radar and communication design: Applications, state-of-the-art, and the road ahead," *IEEE T COMMUN*, vol. 68, no. 6, pp. 3834–3862, 2020.

[3] H. Guo, Y.-C. Liang, J. Chen *et.al.*, "Weighted sum-rate maximization for reconfigurable intelligent surface aided wireless networks," *IEEE Trans. Wireless Commun.*, vol. 19, no. 5, pp. 3064–3076, 2020.

[4] C. Pan, H. Ren, K. Wang *et.al.*, "Reconfigurable intelligent surfaces for 6G systems: Principles, applications, and research directions," *IEEE Commun. Mag.*, vol. 59, no. 6, pp. 14–20, 2021.

[5] Z.-M. Jiang, M. Rihan, P. Zhang *et.al.*, "Intelligent reflecting surface aided dual-function radar and communication system," *IEEE Syst. J.*, vol. 16, no. 1, pp. 475–486, 2022.

[6] R. Liu, M. Li, H. Luo *et.al.*, "Integrated sensing and communication with reconfigurable intelligent surfaces: Opportunities, applications, and future directions," *IEEE Wireless Commun.*, vol. 30, no. 1, pp. 50–57, 2023.

[7] K. Zhi, C. Pan, H. Ren *et.al.*, "Active ris versus passive ris: Which is superior with the same power budget?" *IEEE Communications Letters*, vol. 26, no. 5, pp. 1150–1154, 2022.

[8] Z. Zhang, L. Dai, X. Chen *et.al.*, "Active RIS vs. passive RIS: Which will prevail in 6G?" *IEEE Trans. Commun.*, vol. 71, no. 3, pp. 1707–1725, 2023.

[9] Q. Zhu, M. Li, R. Liu *et.al.*, "Joint transceiver beamforming and reflecting design for active RIS-aided ISAC systems," *IEEE Trans. Veh. Technol.*, vol. 72, no. 7, pp. 9636–9640, 2023.

[10] A. A. Salem, M. H. Ismail, and A. S. Ibrahim, "Active reconfigurable intelligent surface-assisted MISO integrated sensing and communication systems for secure operation," *IEEE Trans. Veh. Technol.*, vol. 72, no. 4, pp. 4919–4931, 2023.

[11] R. P. Sankar and S. P. Chepuri, "Beamforming in hybrid RIS assisted integrated sensing and communication systems," in *European Signal Proces. Conf. (EUSIPCO)*, 2022, pp. 1082–1086.

[12] P. Tseng, "Convergence of a block coordinate descent method for nondifferentiable minimization," *J. Optim. Theory Appl.*, vol. 109, pp. 475–494, 2001.

[13] Q. Wu and R. Zhang, "Intelligent reflecting surface enhanced wireless network via joint active and passive beamforming," *IEEE Trans. Wireless Commun.*, vol. 18, no. 11, pp. 5394–5409, 2019.